ORIGINAL RESEARCH PAPER

Investigation of Elastic Leak in Rectangular Hydrogel Seals

A.A. Abbasian Arani*, H. Barkhordari

Mechanical Engineering Faculty, University of Kashan, Kashan, Iran.

Article info	Abstract
	Eliminating the need for external manipulation due to the ability of hydrogels to sense the environmental stimuli and swelling, makes it suitable for sealing applications. As the matter of fact, many researchers from both academia and industry have investigated hydrogel seals experimentally and numerically. In this work, by using constitutive models available in the literature, the sealing properties of rectangular hydrogel seals are numerically investigated. To investigate elastic leakage of hydrogel seals subjected to fluid pressure, leakage models of elastomeric ones are implemented. The methods are validated by comparing the result of the model with available experiments in the literature. Afterward, the mechanism of leakage of hydrogel seal is presented, and then, parameter studies are carried out. It has been found that increasing the cross-link density, hydrogel length, and the ratio of hydrogel thickness to the gap it seals increases the value of fluid pressure associated with leakage.

Nomenclature

$\mathbf{F}$	Deformation gradient tensor	$\mathbf{C}$	Right Cauchy-green deformation tensor
W	Free energy density	χ	Interaction parameters
W_e	Elastic free energy density of the network	C	Concentration of water molecules
W_m	Mixing free energy density of the network	T	Temperature
α	Governing equation constant	RTG	Ratio of hydrogel thickness to the gap
v	volume of a water molecule	$\mathbf{P}$	First Piola-Kirchoff stress tensor
k	Boltzmann constant	μ	Chemical potential
I	First invariant of $\mathbf{C}$	σ_c	Contact stress
J	Determinant of deformation gradient tensor	$\mathbf{X}$	Coordinate of the element of the network at initial position
N	Cross-linking density of the hydrogel network	$\mathbf{x}(\mathbf{X})$	Coordinate of the element of the network at current position

1. Introduction

Long-chain hydrophilic polymers connected through cross-linkers form a solid structure are known as hydrogel. Hydrogels have the unique ability to absorb solvents up to hundreds of times their initial volume and are highly practical. Thus, they have attracted the attention of many researchers in recent years. Hydrogels have applications in drug delivery systems [1], tissue engineering [2], sensing and actuating devices [3, 4], microfluidics [5–10], and seals (which is the focus of this work) [11–14].

Sealing is one of the most important applications of

elastomers [15]. Elastomeric seals are placed in a gap between two hard materials to prevent fluid to pass through the gap. An elastomer in the desired place should be compressed to produce contact stress and act as a seal. Otherwise, the fluid leaks through the gap [16]. Hydrogels have recently been used as seals. Due to their ability to absorb surrounding solvents and swelling, they are able to automatically produce the necessary contact stress [17]. This application of hydrogels has attracted the attention of researchers in both academia [11, 15, 17] and industry [12, 18], and there has been a great deal of interest in their industrial applications as seals. In their pioneer work, Beebe et al. [11] introduced a pH-responsive valve to regulate fluid in microfluidic devices. Furthermore, patents [19–21] have introduced methods of improving their functionality.

In the present study, rectangular sealing systems are comprehensively investigated and discussed. This system is shown in Fig. 1. When placed in the required location, the hydrogel swells by absorbing the surrounding water and provides the contact stress required for sealing. The advantage of this system is its ease of use and low cost compared to traditional sealing methods. In traditional systems, one side of the sealing portion should be mobile to be pressed toward the elastomer and build the contact stress. On the contrary, as hydrogels can absorb water and swell, they automatically generate this contact stress.
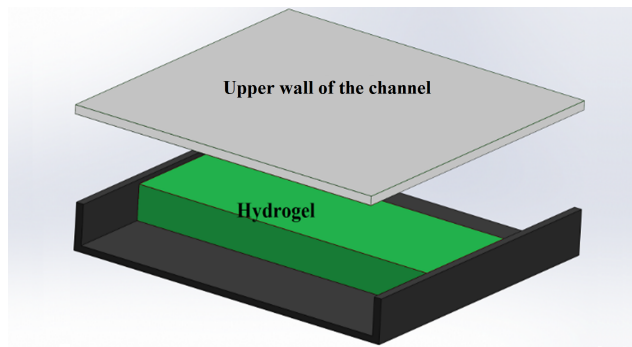

Fig. 1. Schematic of a rectangular seal made of hydrogel inside a channel.

Even though seals are not expensive, their failure might turn out so [15]. Therefore, the design stage of such a device is of essential importance. Researchers have studied hydrogel seals from different points of view. The fundamental mechanism of leakage in these seals have been investigated in [15, 17, 22]. Thermomechanical material models of hydrogels have been employed to study the kinetics of swelling and contact stress built-up of such materials in sealing devices [12, 23–26]. Geometrical parameters effects on the hydrogel contact stress produced by its swelling have been addressed in [27]. However, none of these works have studied the swelling, consequent sealing, and leakage of hydrogel seals. This study aims to investigate the

performance of hydrogel seals and to investigate different parameters involved to present a reliable guide for designing such seals.

The coupled nonlinear model of the elastomeric hydrogels has attracted the attention of researchers [28–31]. A constitutive model is necessary to predict the behavior of a hydrogel in complicated thermo-mechanical conditions. In seals, the swelling of the hydrogel and its contact with the channel wall that produces the necessary contact stress is a complex phenomenon. Therefore, a coupled thermo-mechanical model is required to predict the performance of a hydrogel seal. Hong et al. [29] introduced a model considering fluid permeation and large deformation of solids. They followed the assumption of Flory and Rehner [32] that the free energy of the hydrogel consists of two parts: mixing of solvent and polymer chains and stretching of the network. They used the Flory-Huggins [33, 34] and neo-Hookean models for these two parts, respectively.

This article is structured as follows. After the introduction in Section 1, the material thermo-mechanical model and mechanism of leakage are described in Section 2. In Section 3, the models are validated in comparison with experiments available in the literature. In section 4, a complete investigation of a seal is presented. Various parameters are discussed in section 5. Finally, in Section 6, the results and conclusions are presented.

2. Models

2.1. Hydrogel Constitutive Model

A hydrogel network in its dry state is considered as the reference state, and the coordinate of its element is denoted by $\mathbf{X}$. In the deformed state, element coordinate and deformation gradient are expressed by $\mathbf{x}(\mathbf{X})$ and $\mathbf{F}$, respectively. It should be noted that this paper uses Lagrangian formulation.

The hydrogel network is modeled as a hyperelastic material. The model introduced by [29] is used to model the hydrogel behavior. This model is based on the additive decomposition of the free energy which takes the form [32]:

$$W(\mathbf{F}, C) = W_m(C) + W_s(\mathbf{F}) \tag{1}$$

where W_m is the free energy density from the mixing of the solvent and polymer chains, W_s is free energy density from the stretch of the chains, and C is the concentration of water molecules. The mixing part of the free energy density is based on the mentioned references [33, 35]:

$$W_m(C) = -\frac{kT}{\nu} \left[\nu C \ln\left(1 + \frac{1}{\nu C}\right) + \frac{\chi}{1 + \nu C} \right] \tag{2}$$

where k, T, ν, and χ are Boltzmann constant, temperature, volume per molecule, and interaction parameter, respectively. The first part of this equation, i.e., the logarithm part, refers to the entropy of water-polymer mixing and the second from the enthalpy of mixing. χ is a dimensionless parameter with representative values of $\chi = 0 - 1.2$ [36]. Note that lower values of χ motivate the fluid molecules to enter the network.

A neo-Hookean model is employed for the free energy changes due to the deformation of the hydrogel:

$$W_s(\mathbf{F}) = \frac{1}{2}NKT(I_1 - 3 - 2\ln J) \qquad (3)$$

where N, I_1, and J are the concentration of polymer chains, first invariant of the right Cauchy–Green deformation gradient[1], and the determinant of deformation gradient, respectively. Note that when hydrogel is in the dry state, NKT is equal to its shear modulus of and has representative values of $NKT = 1\text{kPa} - 10\text{MPa}$ [36].

As both fluid molecules and polymer chains are incompressible, the state equation (at equilibrium) for hydrogel at any chemical potential of fluid is obtained as [29]:

$$\mathbf{P} = \frac{\partial W}{\partial \mathbf{F}} - \frac{\mu}{\nu}\mathbf{I} \qquad (4)$$

where $\mathbf{P}$, $\mathbf{I}$, and μ are the first Piola-Kirchoff stress tensor, the identity tensor, and the chemical potential of the surrounding fluid, respectively. Negative chemical potential imposes hydrostatic stress term on the network, also known as pore pressure in poroelasticity. This way, the chemical potential affects the final volume of the network. When the pressure of the fluid is equal to vapor pressure at equilibrium, the chemical potential is zero.

As hydrogel is immersed in water, the molecules start to migrate into the network, and the hydrogel swells. This happens only when the polymer chains stretch to accommodate the water molecules. This stretch reduces the entropy of the polymer chains, creating contractile stress. Moreover, the mixing changes the entropy and enthalpy of the system. At equilibrium state, a balance exists in the hydrogel between all these effects and the chemical potential and mechanical load.

The model is implemented in ABAQUS by a user-defined material subroutine (UHYPER) to solve problems with complicated boundary conditions. For this purpose, the free energy derivatives of the model are calculated and introduced into the subroutine.

2.2. Mechanism of Leakage

Failure of elastomeric seals has three modes [22]. One is the elastic escape which occurs mostly in O-rings. In this mode of failure, the seal escapes from the sealing site into the tight gap that it seals. The second failure mode occurs following the rupture of the elastomer. The rupture creates a crack in the elastomer, and leakage occurs through this crack. This crack could be either local or a front-to-end crack. The third failure mode is the elastic leak, which is the focus of this work. In this mode, the elastomer is not damaged or removed from the sealing site, and its elastic deformation causes the failure. Note that seals can prevent leakage by exerting contact stress on the wall than is higher than the surrounding pressure. Following deformation, the value of fluid pressure may exceed this contact stress that the seal put on the channel wall, and the seal cannot prevent the fluid from passing through the gap. The elastic leak is considered as a reversible process. As the pressure difference is removed, the elastomer returns to the its initial configuration.

In a channel containing water, the hydrogel swells and impacts the channel wall, thus creating the necessary contact stress and sealing the channel. At this initial state, the distribution of the contact stress is symmetrical. The stress peaks at the middle of the hydrogel length and disappears at the two contacting ends. When the pressure on one side of the seal increases, the hydrogel deforms, and the distribution of the contact stress changes. The peak of the contact stress relocates and approaches the side with higher pressure. In addition, the contact stress at the high-pressure side increases but remains zero on the other side. As the pressure difference increases, the peak further approaches the contact edge. In some cases, at a specific value of pressure, the peak reaches the contact edge. In this case, if the peak value does not match the fluid pressure (the stress is higher than the pressure) as the pressure rises the magnitude of contact stress at the peak rises too, but not as much as the pressure, so at some point, the pressure will exceed the peak and will form a leaking path [15]. If the contact edge does not coincide with the hydrogel edge and the contact stress peak equals the fluid pressure, the seal fails [37]. If the pressure difference is removed, the hydrogel returns to the initial state because of the reversibility of the elastic deformation. Therefore, the mechanism of the elastic leak is considered as a reversible phenomenon.

3. Validation

The models established in the previous section are validated by examining a rectangular seal similar to Fig. 1 which were studied in [15] using FEA. As illustrated in Fig. 1, the sealing system is composed of the hydrogel body with dimensions of h, l, and w and a channel with an adjustable upper cover. The bottom surface of the hydrogel is glued to the channel. The chan-

---

[1] Note that the right Cauchy–Green deformation gradient is defined as $\mathbf{C} = \mathbf{F}^T\mathbf{F}$.

nel width has sufficient length to model the system as two-dimensional one. Adjusting the upper cover of the channel applies compression to the hydrogel so it can perform as a seal (this mimics the swelling of hydrogel - the authors did so to avoid the very long swelling time). The level of compression is of major importance; higher compression of the hydrogel requires higher fluid pressure to cause leakage. The strain of compression (ε) is the dimensionless parameter of the amount of compression, defined as $\Delta h/h$. Experimental investigations of this system are presented in [15]. The study also introduces an approximate analytical solution.

Since there is no swelling in the seal of the intended test, a neo-Hookean model is adopted for modeling the deformation. The upper boundary is a rigid line that moves downward and makes contact with the elastomer and compresses it. The contact is considered to be frictionless which is following the real experiment as it is stated in the paper that the contact is almost frictionless [15]. The mesh type for the elastomer and moving boundary are R2D2 and CPE4H, respectively. The water pressure is modeled as a uniform pressure on the left side of the rectangular, and it rises linearly until reaching the maximin contact stress. At first, however, it is not fully compatible with the experiment since, in the real scenario, water puts pressure on all contactless areas. Nonetheless, this is not a problem since after a short time, all part of the upper side of the seal becomes in contact with the boundary and only the left side remains in contact with water. The water pressure and contact stress are constantly mentioned, and when water pressure exceeds the value of contact stress the leakage is reported.

Herein, FEA of the seal was conducted, and results were compared with the results of the both experiments and analytical solutions. The dimensions and parameters of the process are as follows: $N\nu = 0.000125$, $\varepsilon = 10\%$, the height of the hydrogel=1cm, and three different lengths of the hydrogel, 2.2, 4.4, and 6.7cm. Note that the friction of the upper cover of the channel is taken to be frictionless.

Fig. 2a-d shows the shape of the seal with a length of 6.7cm under various pressures. Additionally, Fig. 2e shows seal contact stresses at various pressures corresponding to (a)-(d). In Fig. 2a, the upper cover is lowered to apply compression to the hydrogel. In Fig. 2b-d, the pressure is applied to the left side of the hydrogel, leading to deformation and increasing the contact stress. Contact stress was at its peak in the middle of the hydrogel. After applying pressure on one end of the hydrogel, the peak increases and approaches the high-pressure end until it reaches the end point of the hydrogel. After it has reached the end point of the hydrogel, the peak only grows in magnitude. This process is slower than the increase in fluid pressure and continues until the applied fluid pressure exceeds the contact stress and leakage initiates. At a pressure difference of 186kPa, leakage initiates. Table 1 shows the result of FEA and experiments and the analytical solution presented in [1] for various dimensions. Considering the nature of the materials and the application, the results of FEA are in acceptable agreement with results of the experiments and the approximate analytical solution. Models for hydrogel usually have a considerable deviation from experiments as their behavior has many aspects that cannot be captured in the models. Moreover, the leakage is unstable in nature, and its precise prediction is not possible.

Table 1
Comparison of leakage pressure obtained from experiments, approximate analytical solution and FEA for the rectangular seal.

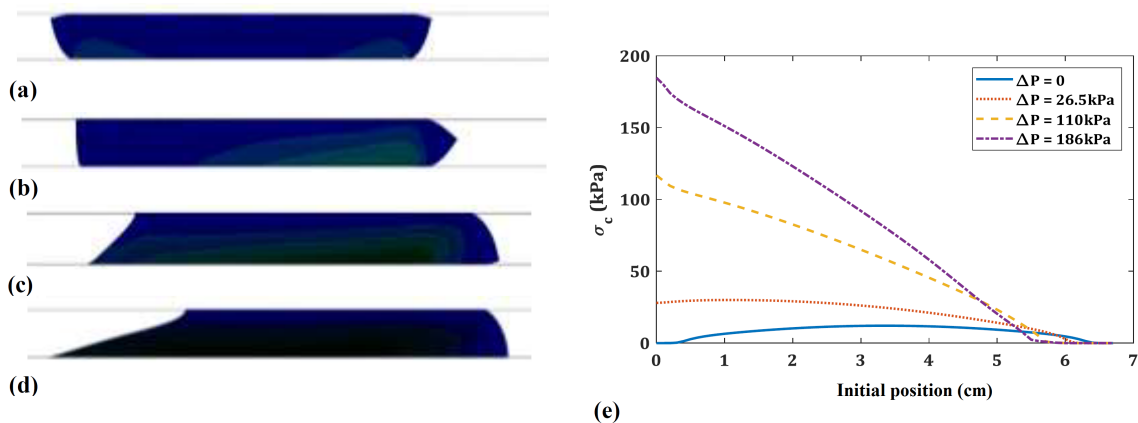| l/h	P_l from experiment [18] (kPa)	P_l from analytical solution [15] (kPa)	P_l from FEA (kPa)
2.2	38.8	44.4	43.4
4.4	110.5	104.5	108.5
6.7	174.5	184	186

(a)

(b)

(c)

(d)

(e)

Fig. 2. FEA of the rectangular seal subjected to various pressure differences in the channel. (a)-(d) Shape of the seal at different ΔPs of 0, 26.5kPa, 110kPa, and 186kPa (the instance of leakage), respectively. e) Plot of the contact stress corresponding to (a)-(d).

4. Detailed Investigation of a Rectangular Hydrogel Seal

This paper uses FEM to investigate the problem. The UHYPER subroutine was developed to introduce the material model to ABAQUS software. The energy parameter and its derivative with respect to the deformation gradient invariants were scripted in the UHYPER. In ABAQUS software, the CPE4H mesh model is used to simulate the problem as the seal length is considered sufficient as a 2D problem (Fig. 2a-d). The FE model is similar to the validation model explained earlier, except for the material model of hydrogel instead elastomer and the movement of the upper boundary condition.

The investigated hydrogel had a length of 27.5mm and thickness of 11mm and was placed in a 15-mm channel. The material properties are as follows: the crosslink density is 0.01, and the interaction parameter is 0.6. Fig. 3 shows the different steps of the system configuration. Fig. 3a illustrates the hydrogel when initially placed in the channel before swelling. In Fig. 3b, the hydrogel swelling is complete, but no pressure difference was applied. In Figs. 3c to f, the pressure differences of 600kPa, 1040kPa, 1920kPa, and 2915kPa are applied to one side of the hydrogel. Note that leakage has occurred in (f), and the elastic leak has led to system failure. Furthermore, these images show the von Mises stress contour. After swelling and before applying fluid pressure (Figure (b)), the stress is maximum at the two lower corners glued to the wall. Initially, the maximum value on the high-pressure side decreases with applying the fluid pressure (Figs. 3c and d) and then starts to increase. This is due to the hydrogel deformation.
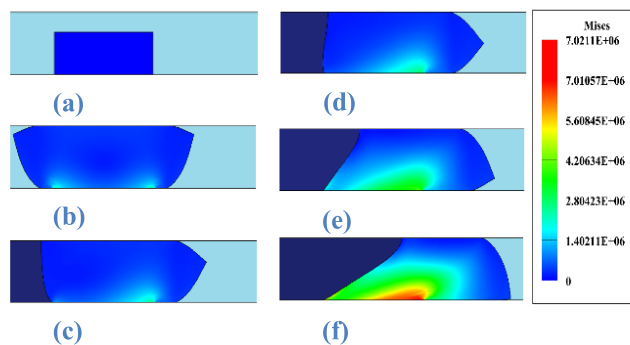

Fig. 3. Von Misses stress inside the hydrogel at different pressures.

When the fluid pressure rises, elements in this corner approach their initial position, so their stretches decrease. However, at a specific point, these elements begin to distance, and their stretch extends again.; therefore, their stresses start to rise again. In the low-pressure corner, von Mises stress is constantly increasing and is practically the constant critical point.

The contact stress between the hydrogel and the channel wall is illustrated in Fig. 4 to investigate the subject further. In the instances where contact stress is plotted, the pressure difference is similar to Fig. 4. Initially, the contact stress profile is perfectly symmetrical. In the center of the hydrogel, the contact stress is maximum and is zero at the two contact ends. Note that initially, the contact end does not coincide with the hydrogel corner, meaning that parts of the outer hydrogel surface are not in contact with the wall. Under increasing pressure, the hydrogel slowly deforms, and before the fluid pressure reaches the maximum contact stress, this maximum point moves to the hydrogel corner. After the hydrogel corner reaches the wall and corresponds to the location of the maximum contact stress, the pressure increases with a sharper slope than in other areas. As a result, although the contact stress is lower than the fluid pressure in most contact areas, the hydrogel prevents leakage as the contact stress in this area is higher than the fluid pressure. When the contact stress of this area falls below the external pressure, the system fails, and leakage begins. This sudden leak was also observed in the experiments [15, 17]. Another effect of deformation is the reduction of the contact on the low-pressure side. Higher pressure difference and deformation mean that the contact surface of the hydrogel and the low-pressure wall are smaller.
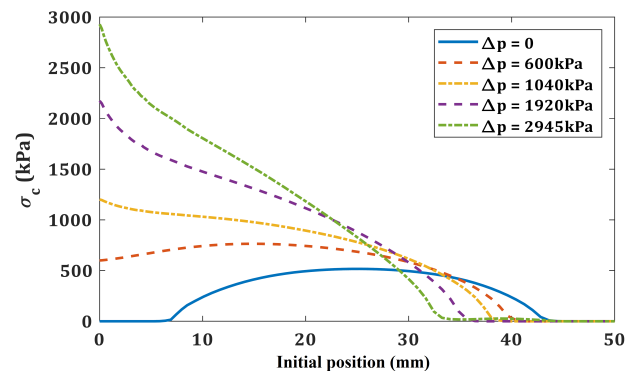

Fig. 4. Contact stress of the hydrogels at different pressures according to Fig. 3.

5. Parameter Study

This section investigates the essential parameters of the sealing system. The parameters are cross-linking density of the hydrogel ($N\nu$), length of the hydrogel, and the ratio of hydrogel thickness to the gap that seals (RTG). As stated in the model description, cross-linking density is an essential parameter in hydrogel behavior and has a large impact on the amount of swelling and contact stress, among others. Length of the hydrogel is investigated as more contact means a larger area for contact stress and resistance to deformation. RTG is studied because the thickness of the hydrogel controls the initial contact stress. Moreover, some systems contain barriers that prevent the designer from choosing the thickness of the hydrogel.

5.1. Cross-linking Density

As discussed in the model description, cross-linking density has a considerable effect on the equilibrium swelling ratio and the stress generated by the material. Additionally, it can be easily controlled by adding cross-linkers to the network when synthesizing the hydrogel. Therefore, this section investigates the results of this essential parameter in hydrogel swelling and sealing. In this study, hydrogel length, height, interaction parameter, and channel height are 25mm, 10mm, 0.6, and 15mm, respectively.
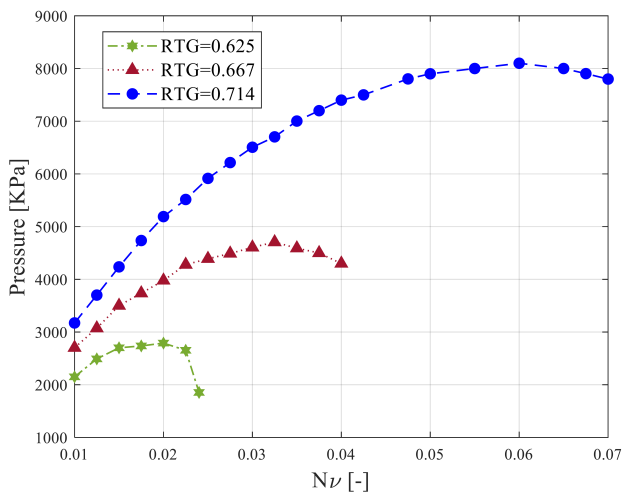

Fig. 5. Effect of cross-linking density on maximum tolerable pressure.

In the study of the effects of this parameter on the leakage, three RTG values are used to consider the multiplicative effect of these parameters (Fig. 5). As shown in the diagram, the difference in tolerable final pressure initially increases with increasing $N\nu$. At a specific point, however, this increase stops, and the tolerable final pressure difference decreases with increasing $N\nu$. This trend can be seen with all three RTG values, with the difference that for higher RTG values, this phenomenon also occurs in higher values of $N\nu$.

Cross-linking density affects contact stress in two ways. First, a larger $N\nu$ is equivalent to a larger shear modulus, meaning that more stress is needed to create deformation. Second, lower $N\nu$ causes more extensive swelling, meaning that swelling is limited by the wall. This confinement necessitates higher stress. These two factors are in behavioral conflict. This conflict increases the bearing pressure of the system, which then decreases as the $N\nu$ increases.

The cross-linking density of the maximum tolerable pressure tends to increase with higher RTG. This is because the first factor is more effective when the hydrogel is closer to the wall.

5.2. Hydrogel Length

This section investigates the effect of hydrogel length on system behavior. The results are presented in Fig. 6. In this study, hydrogel height, interaction parameter $N\nu$, and channel height are 10mm, 0.6, 0.01, and 15mm, respectively. According to Fig. 6, as the hydrogel length increases, its ability to withstand the pressure difference increases in an almost linear way. This increase is the possible result of the deformation of the hydrogel. Longer hydrogel has a higher resistance to deformation. In resisting deformation, the hydrogel pressure on the wall increases, and higher contact stress is created. This creates a higher-pressure difference. As shown in Fig. 6, doubling the hydrogel length increases the tolerable pressure almost three times.
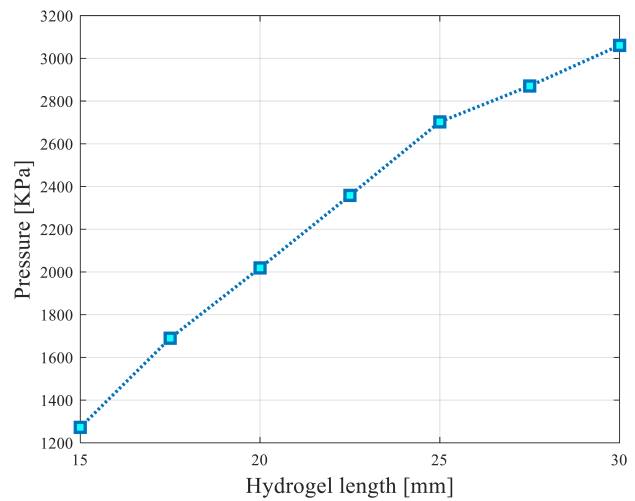

Fig. 6. Effect of hydrogel length on maximum tolerable pressure.

5.3. The Ratio of Hydrogel Thickness to the Gap (RTG)

RTG is an essential operational parameter. In practice, this parameter is governed by the equipment and situation of the place of the hydrogel. Since the channel dimensions are known, the RTG parameter depends on the hydrogel thickness. Fig. 7 shows the results of the investigation of this parameter. Furthermore, the RTG study was performed on three different values of $N\nu$ to investigate its multiplicative effects. In this study, hydrogel length, interaction parameter, and channel height are 25mm, 0.6, and 15mm, respectively.

With lower RTG values, hydrogel swelling is not sufficient to reach the wall. The contact initiates at higher RTG values. After contact and the creation of initial contact stress, one of the two described failure modes might occur. At low RTG values, leakage occurs before the maximum stress reaches the hydrogel corner. In this mode, the tolerable pressure difference

is relatively small. At larger RTG values, the maximum contact stress reaches the hydrogel corner, and the system is capable of tolerating significantly larger pressures. The reason is that when maximum stress reaches the corner, its pressure on the wall increases significantly and creates a sharp slope in contact stress (Fig. 4). In both failure modes, the tolerable pressure can be increased by increasing the RTG.
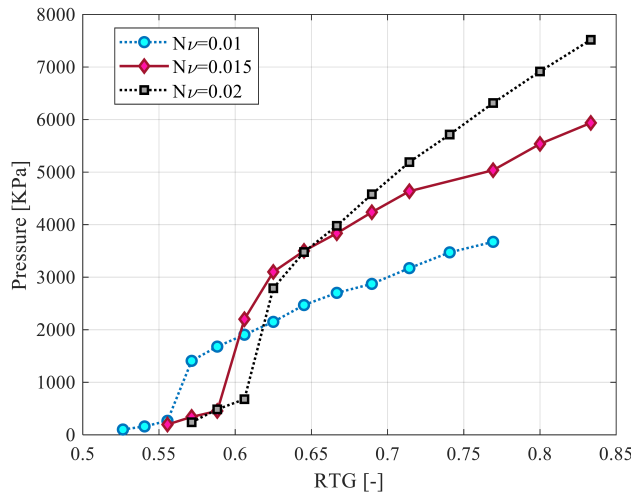

Fig. 7. Effect of RTG on maximum tolerable pressure.

Three different $N\nu$ values were studied to investigate its multiplicative effect. It is observed that the transition between the two failure states occurs at a lower RTG for smaller $N\nu$. This means that a hydrogel with a lower $N\nu$ is better for sealing channels with larger gaps. On the other hand, with larger RTGs, where all three cases pass the transition, the larger $N\nu$ can better seal the channel.

6. Conclusions

This paper studied the behavior of hydrogel seals. First, a model was presented to predict the behavior of hydrogels, and another model suitable for the elastic leak was introduced. Both models were validated through experiments. Afterward, the models were used to examine the leakage of a seal thoroughly. It included the deformation, the stresses created in the hydrogel, contact stress, and the essential operating parameter, i.e., the pressure difference tolerated before failure. Then, a parameter study was conducted to demonstrate the design of these seals. Hydrogel length, cross-linking density, and the geometric parameter of the ratio of the thickness of the hydrogel to the gap (RTG) were the parameters considered in this paper. The results showed that as the hydrogel seal length increases, the pressure-bearing capacity increases, and a larger RTG mean a higher tolerable pressure difference. However, the value of $N\nu$ depends on the situation; to

a specific point, the tolerable pressure increases with increasing $N\nu$ but then decreases.

References

[1] N.A. Peppas, J.Z. Hilt, A. Khademhosseini, R. Langer, Hydrogels in biology and medicine: from molecular principles to bionanotechnology, Adv. Mater., 18(11) (2006) 1345-1360.

[2] G. Chan, D.J. Mooney, New materials for tissue engineering: towards greater control over the biological response, Trends Biotechnol., 26(7) (2008) 382-392.

[3] L. Dong, A.K. Agarwal, D.J. Beebe, H. Jiang, Adaptive liquid microlenses activated by stimuli-responsive hydrogels, Nature, 442(7102) (2006) 551-554.

[4] C. Yang, W. Wang, C. Yao, R. Xie, X.J. Ju, Z. Liu, L.Y. Chu, Hydrogel walkers with electro-driven motility for Cargo transport, Sci Rep, 5 (2015) 13622.

[5] A. Ghasemkhani, H. Mazaheri, A. Amiri, Fluid-structure interaction simulations for a temperature-sensitive functionally graded hydrogel-based micro-channel, J. Intell. Mater. Syst. Struct., 32(6) (2020) 661-677.

[6] H. Mazaheri, A. Khodabandehloo, FSI and non-FSI studies on a functionally graded temperature-responsive hydrogel bilayer in a micro-channel, Smart Mater. Struct., 31(1) (2022) 015007.

[7] H. Mazaheri, A. Ghasemkhani, S. Sabbaghi, Study of fluid–structure interaction in a functionally graded pH-sensitive hydrogel micro-valve, Int. J. Appl. Mech., 12(05) (2020) 2050057.

[8] H. Mazaheri, K. Soleymani, A. Ghasemkhani, An analytical solution and FEM simulation for the behavior of sensitive FG micro-valve in response to pH stimuli, J. Stress Anal., 6(1) (2021) 157-166.

[9] H. Mazaheri, A. Khodabandehloo, Behavior of an FG temperature-responsive hydrogel bilayer: Analytical and numerical approaches, Compos. Struct., 301 (2022) 116203.

[10] H. Mazaheri, A. Ghasemkhani, Analytical and numerical study of the swelling behavior in functionally graded temperature-sensitive hydrogel shell, J. Stress Anal., 3(2) (2019) 29-35.

[11] D.J. Beebe, J.S. Moore, J.M. Bauer, Q. Yu, R.H. Liu, C. Devadoss, B.H. Jo, Functional hydrogel structures for autonomous flow control inside microfluidic channels, Nature, 404(6778) (2000) 588-590.

[12] Y. Lou, S. Chester, Kinetics of swellable packers under downhole conditions, Int. J. Appl. Mech., 06(06) (2014) 1450073.

[13] D. Kim, D.J. Beebe, A bi-polymer micro one-way valve, Sens. Actuators, A, 136(1) (2007) 426-433.

[14] H. Mazaheri, A.H. Namdar, A. Amiri, Behavior of a smart one-way micro-valve considering fluid–structure interaction, J. Intell. Mater. Syst. Struct., 29(20) (2018) 3960-3971.

[15] Q. Liu, Z. Wang, Y. Lou, Z. Suo, Elastic leak of a seal, Extreme Mech. Lett., 1 (2014) 54-61.

[16] B. Lorenz, B.N.J. Persson, Leak rate of seals: Comparison of theory with experiment, Europhys. Lett., 86(4) (2009) 44006.

[17] B. Druecke, E.B. Dussan V., N. Wicks, A.E. Hosoi, Large elastic deformation as a mechanism for soft seal leakage, J. Appl. Phys., 117(10), (2015) 104511.

[18] T.T. Hailey Jr, Freyer, Well tools with actuators utilizing swellable materials, Google Patents, US8453746B2, (2013).

[19] E.R. Abi Aad, Swellable packer, Google Patents, 9441449 (2016).

[20] J. Kluge, B. Jansen, A. Lutz, D.K. De, W.S. Butterfield, P. Williamson, Downwell system with activatable swellable packer, Google Patents, 20090205841 (2009).

[21] E.J. Gustafson, W.S. Butterfield, P. Williamson, Downwell system with differentially swellable packer, Google Patents, 20090205817 (2009).

[22] Z. Wang, C. Chen, Q. Liu, Y. Lou, Z. Suo, Extrusion, slide, and rupture of an elastomeric seal, J. Mech. Phys. Solids, 99 (2017) 289-303.

[23] Q. Liu, A. Robisson, Y. Lou, Z. Suo, Kinetics of swelling under constraint, J. Appl. Phys., 114(6) (2013) 064901.

[24] A.H. Namdar, H. Mazaheri, Kinetics of swelling of cylindrical temperature-responsive hydrogel: a semi-analytical study, Int. J. App. Mech., 12(08) (2020) 2050090.

[25] A.H. Namdar, Kinetics of swelling of cylindrical functionally graded temperature-responsive hydrogels, J. Comput. Appl. Mech., 51(2) (2020) 464-471.

[26] H. Mazaheri, A. Ghasemkhani, A. Namdar, Behavior of photo-thermal sensitive polyelectrolyte hydrogel micro-valve: analytical and numerical approaches, J. Stress Anal., 5(1) (2020) 21-30.

[27] Y. Lou, A. Robisson, S. Cai, Z. Suo, Swellable elastomers under constraint, J. Appl. Phys., 112(3) (2012) 034906.

[28] S.A. Chester, L. Anand, A coupled theory of fluid permeation and large deformations for elastomeric materials, J. Mech. Phys. Solids, 58(11) (2010) 1879-1906.

[29] W. Hong, X. Zhao, J. Zhou, Z. Suo, A theory of coupled diffusion and large deformation in polymeric gels, J. Mech. Phys. Solids, 56(5) (2008) 1779-1793.

[30] F.P. Duda, A.C. Souza, E. Fried, A theory for species migration in a finitely strained solid with application to polymer network swelling, J. Mech. Phys. Solids, 58(4) (2010) 515-529.

[31] H. Mazaheri, A.H. Namdar, A. Ghasemkhani, A model for inhomogeneous large deformation of photo-thermal sensitive hydrogels, Acta Mech., 232 (2021) 2955-2972.

[32] P.J. Flory, J. Rehner Jr, Statistical mechanics of cross-linked polymer networks II. swelling, J. Chem. Phys., 11(11) (1943) 521-526.

[33] P.J. Flory, Thermodynamics of high polymer solutions, J. Chem. Phys., 10(1) (1942) 51-61.

[34] M.L. Huggins, Some properties of solutions of long-chain compounds, J. Phys. Chem., 46(1) (1942) 151-158.

[35] M.L. Huggins, Solutions of long chain compounds, J. Chem. Phys., 9(5) (1941) 440.

[36] W. Hong, Z. Liu, Z. Suo, Inhomogeneous swelling of a gel in equilibrium with a solvent and mechanical load, Int. J. Solids Struct., 46(17) (2009) 3282-3289.

[37] A. Karaszkiewicz, Geometry and contact pressure of an O-ring mounted in a seal groove, Ind. Eng. Chem. Chem. Res., 29(10) (1990) 2134-2137.